Available online at www.sciencedirect.com
SCIENCE DIRECT
Fuel 85 (2006) 944–956
FUEL
www.fuelfirst.com

The combustion of kerosene: Experimental results and kinetic modelling using 1- to 3-component surrogate model fuels

Philippe Dagaut *, Abderrahman El Bakali [1], Alain Ristori [2]

CNRS Laboratoire de Combustion et Systèmes Réactifs, 1C, Avenue de la Recherche Scientifique, 45071 Orléans Cedex 2, France

Received 19 May 2005; received in revised form 11 October 2005; accepted 12 October 2005
Available online 8 November 2005

Abstract

The oxidation of kerosene Jet-A1 and that of *n*-decane have been studied experimentally in a jet-stirred reactor at atmospheric pressure and constant residence time, over the high temperature range 900–1300 K, and for variable equivalence ratio ($0.5 \leq \phi \leq 2$). Concentration profiles of the reactants, stable intermediates, and final products have been obtained by probe sampling followed by on-line and off-line GC analyses. The oxidation of neat *n*-decane and of kerosene in these conditions was modeled using a detailed kinetic reaction mechanism (209 species and 1673 reactions, most of them reversible). The present model was successfully used to simulate the structure of a fuel-rich premixed *n*-decane–oxygen–nitrogen flame. In the modelling, kerosene was represented by four surrogate model fuels: 100% *n*-decane, *n*-decane-*n*-propylbenzene (74%/26% mol), *n*-decane-*n*-propylcyclohexane (74%/26% mol), and *n*-decane-*n*-propylbenzene-*n*-propylcyclohexane (74%/15%/11% mol). The 3-component model fuel was the most appropriate for simulating the JSR experiments. It was also successfully used to simulate the structure of a fuel-rich premixed kerosene–oxygen–nitrogen flame.

Keywords: Oxidation; Hydrocarbon; Kinetics; Modelling; Surrogate; Kerosene; Jet-A; JP-8

1. Introduction

Kerosene Jet A1 is a complex mixture of alkanes (50–65% vol.), mono- and poly-aromatics (10–20% vol.) and cycloalkanes or naphtenes (mono- and polycyclic, 20–30% vol.) widely used in aircraft engines. A better knowledge of its kinetic of combustion is of interest for (i) modelling its combustion in aviation turbine engines, and (ii) for safety reasons. Actually, the first issue is addressed through high-pressure studies whereas the second one that covers pool fires must be addressed via atmospheric pressure studies. The compounds identified in Jet-A1 at the highest levels of concentration are *n*-alkanes. Due to the complexity of the composition of this fuel, it is necessary to use a surrogate model fuel for simulating its oxidation. Under high-pressure conditions, the detailed kinetic modelling of kerosene oxidation was initially performed using *n*-decane as a model-fuel [1], since *n*-decane and kerosene had very similar oxidation rates under jet-stirred reactor (JSR) [1–3] and flame conditions[4]. It was clearly shown in a previous work [1] that *n*-decane is an acceptable model fuel for kerosene oxidation under high pressure, if the formation of aromatics is not a major issue since the oxidation of *n*-decane yields much less aromatics that kerosene. Therefore, more complex model fuels are necessary to model the formation of aromatics, key-compounds involved in the formation of PAH and soot, from the oxidation of kerosene. Surrogate model fuels consisting of *n*-decane and mixtures of *n*-decane with simple aromatic and naphtenic hydrocarbons are tested here, mainly under JSR conditions. The detailed kinetic reaction mechanisms for the pure components of the surrogate model fuel had first to be established before merging the sub-mechanisms to yield a kerosene kinetic reaction mechanism. Such a work was partially done previously [5,6] but still needed to be done for *n*-decane. In this paper, we present new experimental results obtained in a JSR for the oxidation of *n*-decane and of kerosene at 1 atm, over a wide range of equivalence ratio (0.5–2), and temperature (900–1300 K). The oxidation of

* Corresponding author. Tel. +33 238 25 54 66; fax +33 238 69 60 04.
E-mail addresses: dagaut@cnrs-orleans.fr (P. Dagaut), abderrahman.el-bakali@univ-lille1.fr (A. El Bakali).
[1] Present address: Université des Sciences et Technologies de Lille, PC2A, UMR CNRS-8522, 59655 Villeneuve d'Ascq Cedex, France
[2] Present address: Faurecia-Exhaust Systems, ITIS/AET/EC, Bois sur Prés, 25550 Bavans, France

0016-2361/$ - see front matter © 2005 Elsevier Ltd. All rights reserved.
doi:10.1016/j.fuel.2005.10.008

Table 1
Rate expressions for pressure dependent reactions ($k = AT^n \exp[-E/RT]$, units: s, mole, cm^3, cal, K)

Reaction	A	n	E	Note
1637. OH + OH(+M) = H_2O_2(+M)	$7.22\times10^{+13}$	−0.4	0.0	a
Low pressure limit:	$0.22\times10^{+20}$	−0.76	0.0	
Troe centering:	$0.50\times10^{+00}$	$0.10\times10^{+09}$	0.10×10^{-05}	
1638. CH_4(+M) = CH_3 + H(+M)	$2.40\times10^{+16}$	0.0	104920.0	b
Low pressure limit:	$0.45\times10^{+18}$	0.0	$0.90815\times10^{+05}$	
Troe centering: $0.64\times10^{+00}$	0.10×10^{-14}	$0.3195\times10^{+04}$	$0.12126\times10^{+05}$	
1639. CH_3 + CH_3(+M) = C_2H_6(+M)	$3.61\times10^{+13}$	0.0	0.0	a
Low pressure limit:	$0.13\times10^{+42}$	$-0.7\times10^{+01}$	$0.2762\times10^{+04}$	
Troe centering:	$0.62\times10^{+00}$	$0.73\times10^{+02}$	$0.118\times10^{+04}$	
1640. H + C_2H_5(+M) = C_2H_6(+M)	$5.21\times10^{+17}$	−1.0	1580.0	c
Low pressure limit:	$0.20\times10^{+42}$	$-0.708\times10^{+01}$	$0.6685\times10^{+04}$	
Troe centering: $0.8422\times10^{+00}$	$0.125\times10^{+03}$	$0.2219\times10^{+04}$	$0.6882\times10^{+04}$	
Third-body efficiencies:	H_2, 2; H_2O, 6;	CH_4, 2; CO, 1.5;	CO_2, 2; C_2H_6, 3.	
1641. C_2H_4 + H(+M) = C_2H_5(+M)	$3.97\times10^{+09}$	1.3	1292.0	a
Low pressure limit:	$0.28\times10^{+19}$	0.0	$0.755\times10^{+03}$	
Troe centering:	$0.76\times10^{+00}$	$0.40\times10^{+02}$	$0.1025\times10^{+04}$	
1642. C_2H_2 + H(+M) = C_2H_3(+M)	$2.34\times10^{+15}$	−0.9	3064.0	d
Low pressure limit: $0.23\times10^{+41}$	$-0.727\times10^{+01}$	$0.658\times10^{+04}$		
Troe centering:	$0.50\times10^{+00}$	$0.675\times10^{+03}$	$0.675\times10^{+03}$	
Third-body efficiencies: H_2, 2;	H_2O, 5;	CO, 2;	CO_2, 3	
1643. H + C_2H(+M) = C_2H_2(+M)	$1.00\times10^{+17}$	−1.0	0.0	c
Low pressure limit:	$0.38\times10^{+34}$	$-0.48\times10^{+01}$	$0.19\times10^{+04}$	
Troe centering: $0.6464\times10^{+00}$	$0.132\times10^{+03}$	$0.1315\times10^{+04}$	$0.5566\times10^{+04}$	
Third-body efficiencies:	H_2, 2; H_2O, 6;	CH_4, 2; CO, 1.5;	CO_2, 2; C_2H_6, 3.	
1644. C_2H_2 + OH(+M) = C_2H_2OH(+M)	$2.29\times10^{+13}$	0.0	1808.0	e
Low pressure limit:	$0.74\times10^{+27}$	$-0.31\times10^{+01}$	$0.18\times10^{+04}$	
Troe centering: $0.17\times10^{+00}$	$0.18\times10^{+03}$	$0.50\times10^{+05}$	$0.12772\times10^{+05}$	
1645. CHOCHO(+M) = CH_2O + CO(+M)	$4.27\times10^{+12}$	0.0	50600.0	f
Low pressure limit:	$0.89\times10^{+17}$	0.0	0.492+05	
1646. CHOCHO(+M) = CO + CO + H_2(+M)	$1.07\times10^{+14}$	0.0	55100.0	g
Low pressure limit:	$0.26\times10^{+17}$	0.0	$0.384\times10^{+05}$	
1647. CH_3 + OH(+M) = CH_3OH(+M)	$5.65\times10^{+13}$	0.1	0.0	h
Low pressure limit:	$0.58\times10^{+42}$	$-0.74\times10^{+01}$	$0.626\times10^{+03}$	
Troe centering: 0.25×10^{-01}	0.10×10^{-14}	$0.80\times10^{+04}$	$0.30\times10^{+04}$	
Third-body efficiencies: H_2, 2;	H_2O, 16;	CO, 2;	CO_2, 3	
1648. C_3H_6 + H(+M) = iC_3H_7(+M)	$5.70\times10^{+09}$	1.2	874.0	i
Low pressure limit:	$0.16\times10^{+55}$	$-0.11\times10^{+02}$	$0.9364\times10^{+04}$	
Troe centering: $0.10\times10^{+01}$	0.10×10^{-14}	$0.26\times10^{+03}$	$0.30\times10^{+04}$	
Third-body efficiencies: H_2, 2;	H_2O, 5;	CO, 2;	CO_2, 3	
1649. C_3H_6 + H(+M) = nC_3H_7(+M)	$1.33\times10^{+13}$	0.0	3260.7	j
Low pressure limit:	$0.63\times10^{+39}$	$-0.666\times10^{+01}$	$0.7\times10^{+04}$	
Troe centering: $0.10\times10^{+01}$	$0.10\times10^{+04}$	$0.131\times10^{+04}$	$0.48097\times10^{+05}$	
Third-body efficiencies: H_2, 2; H_2O, 6;	CH_4, 2;	CO, 1.5;	CO_2, 2.	
1650. nC_3H_7(+M) = C_2H_4 + CH_3(+M)	$1.23\times10^{+13}$	−0.1	30202.0	k
Low pressure limit:	$0.55\times10^{+50}$	$-0.1\times10^{+02}$	$0.35766\times10^{+05}$	
Troe centering: $0.217\times10^{+01}$	0.10×10^{-14}	$0.251\times10^{+03}$	$0.1185\times10^{+04}$	
Third-body efficiencies: H_2, 2;	H_2O, 5;	CO, 2;	CO_2, 3.	
1651. aC_3H_5 + H(+M) ⇔ C3H6(+M)	$3.70\times10^{+14}$	0.0	0.0	j
Low pressure limit:	$0.13\times10^{+61}$	$-0.12\times10^{+02}$	$0.59678\times10^{+04}$	
Troe centering: 0.20×10^{-01}	$0.10966\times10^{+04}$	$0.10966\times10^{+04}$	$0.68595\times10^{+04}$	
1652. pC_3H_4 + OH(+M) ⇒ C3H4OH(+M)	$2.29\times10^{+13}$	0.0	1808.0	l
Low pressure limit:	$0.74\times10^{+27}$	$-0.31\times10^{+01}$	$0.1808\times10^{+04}$	
Troe centering: $0.17\times10^{+00}$	$0.18\times10^{+03}$	$0.50\times10^{+05}$	$0.12772\times10^{+05}$	
1653. $1C_4H_9$(+M) = C_3H_6 + CH_3(+M)	$2.14\times10^{+12}$	0.65	30859.0	m
Low pressure limit:	$6.32\times10^{+58}$	−12.85	355571.0	
Troe centering: $0.371\times10^{+00}$	0.10×10^{-14}	$0.574\times10^{+03}$	$0.2539\times10^{+04}$	
1654. C_2H_3 + C_2H_2(+M) = iC_4H_5(+M)	$1.00\times10^{+04}$	2.4	17900.0	n
Low pressure limit:	$0.26\times10^{+39}$	$-0.741\times10^{+01}$	$0.75\times10^{+04}$	
1655. iC_4H_5(+M) = C_4H_4 + H(+M)	$1.00\times10^{+14}$	0.0	50000.0	o

(*continued on next page*)

Table 1 (*continued*)

Reaction	*A*	*n*	*E*	Note
Low pressure limit:	$0.20\times10^{+16}$	0.0	$0.42\times10^{+05}$	
1656. $nC_4H_5(+M)=C_4H_4+H(+M)$	$1.00\times10^{+14}$	0.0	37000.0	o
Low pressure limit:	$0.10\times10^{+15}$	0.0	0.3+05	
1657. $C_2H_2+nC_4H_5(+M)=C_6H_7c(+M)$	$4.80\times10^{+07}$	0.3	4700.0	n
Low pressure limit:	$0.52\times10^{+26}$	$-0.42\times10^{+01}$	$0.4\times10^{+04}$	
1658. $iC_4H_3(+M)=C_4H_2+H(+M)$	$1.00\times10^{+14}$	0.0	55000.0	o
Low pressure limit:	$0.25\times10^{+16}$	0.0	$0.48\times10^{+05}$	
1659. $nC_4H_3(+M)=C_4H_2+H(+M)$	$1.00\times10^{+14}$	0.0	36000.0	o
Low pressure limit:	$0.10\times10^{+15}$	0.0	$0.3\times10^{+05}$	

Note: (a) Baulch DL, Cobos CJ, Cox RA, Frank P, Hayman G, Just Th, et al. J Phys Chem Ref. Data 1994; 23:847;(b) Cobos CJ, Troe J, Z Phys Chem 1992; 176(2): 161–71; (c) GRI-Mech 2.11; (d) Prada L, Miller JA. Combust Sci Tech 1998; 132:225–50; (e) Fulle D, Hamann HF, Hippler H, Jänsch CP. Ber Bunsenges Phys Chem 1997; 101:1433–42; (f) Marinov NM; Malte PC. Int J Chem Kinet 1995; 27:957–86; (g) Saito K, Kakumoto T, Makami T. J Phys Chem 1984; 88:1182 and (f); (h) Fagerstrom K, Lund A, Mahmoud G, Jodkowski JT, Ratajczak E. Chem Phys Lett 1993; 204:226–34; (i) Seakins PW, Robertson SH, Pilling MJ, Slagle IR, Gmurczyk GW, Bencsura A, et al. J Phys Chem 1993; 97:4450–8; (j) Davis SG, Law CK, Wang H, Combust Flame 1999; 119:375–99; (k) Bencsura A, Knyazev VD, Xing S-B, Slagle IR, Gutman D. Proc Combust Inst 1992; 24:629–35; (l) Assumed similar to C_2H_2+OH; (m) Knyazev VD, Dubinsky IA, Slagle IR, Gutman D. J Phys Chem 1994; 98:11099–108; (n) Wang H, Frenklach M. J Phys Chem 1994; 98:11465–89; (o) Miller JA, Melius CF, Combust Flame 1992; 91:21–39.

n-decane in a JSR and a premixed flame is modelled, validating the kinetic scheme, prior to performing the modelling of kerosene oxidation under JSR and premixed flame conditions using *n*-decane based model fuels.

2. Experimental set-up

The JSR experimental set-up used in this work is that used earlier [5,6]. The reactor consisted of a small sphere of

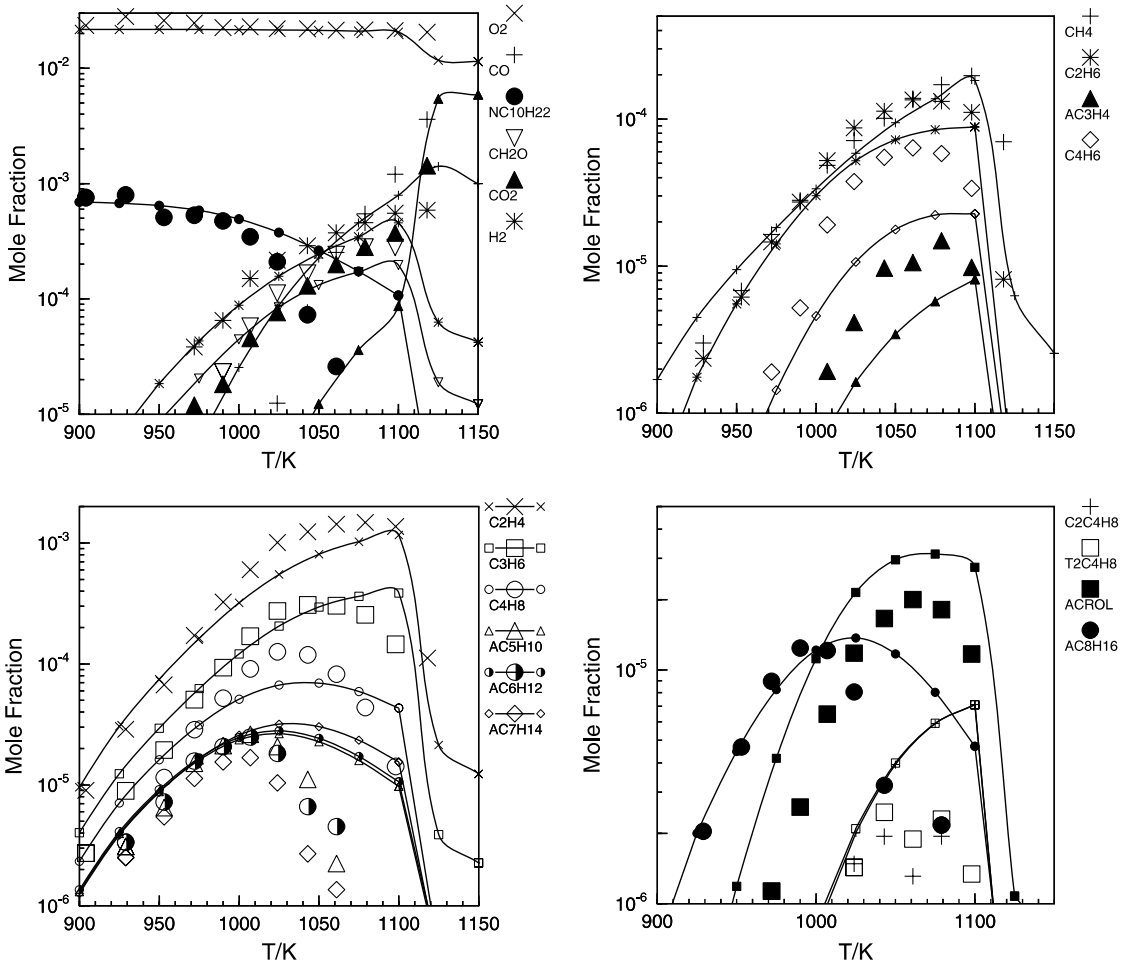

Fig. 1. The oxidation of *n*-decane in a JSR (700 ppmv of *n*-decane, 21700 ppmv of oxygen, nitrogen diluent; 0.07 s, 1 atm). The data (large symbols) are compared to the modeling (lines and small symbols). ACROL stands for acrolein; 1-olefins are named using the prefix A.

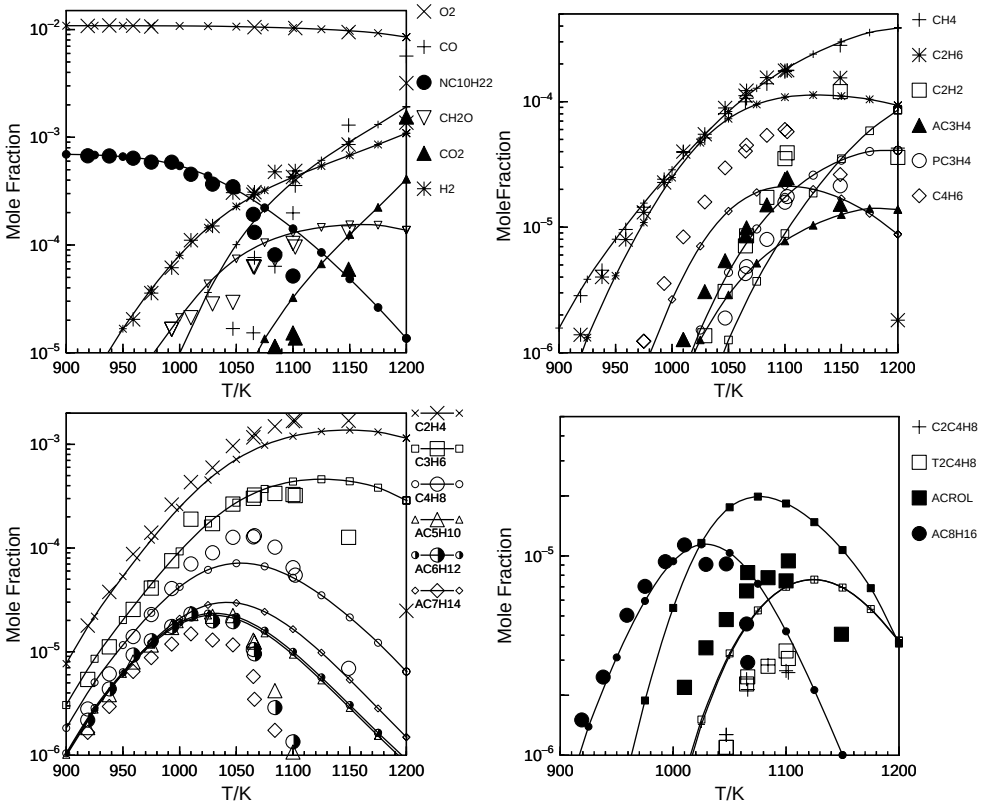

Fig. 2. The oxidation of *n*-decane in a JSR (700 ppmv of *n*-decane, 10,850 ppmv of oxygen, nitrogen diluent; 0.07 s, 1 atm). The data (large symbols) are compared to the modeling (lines and small symbols).

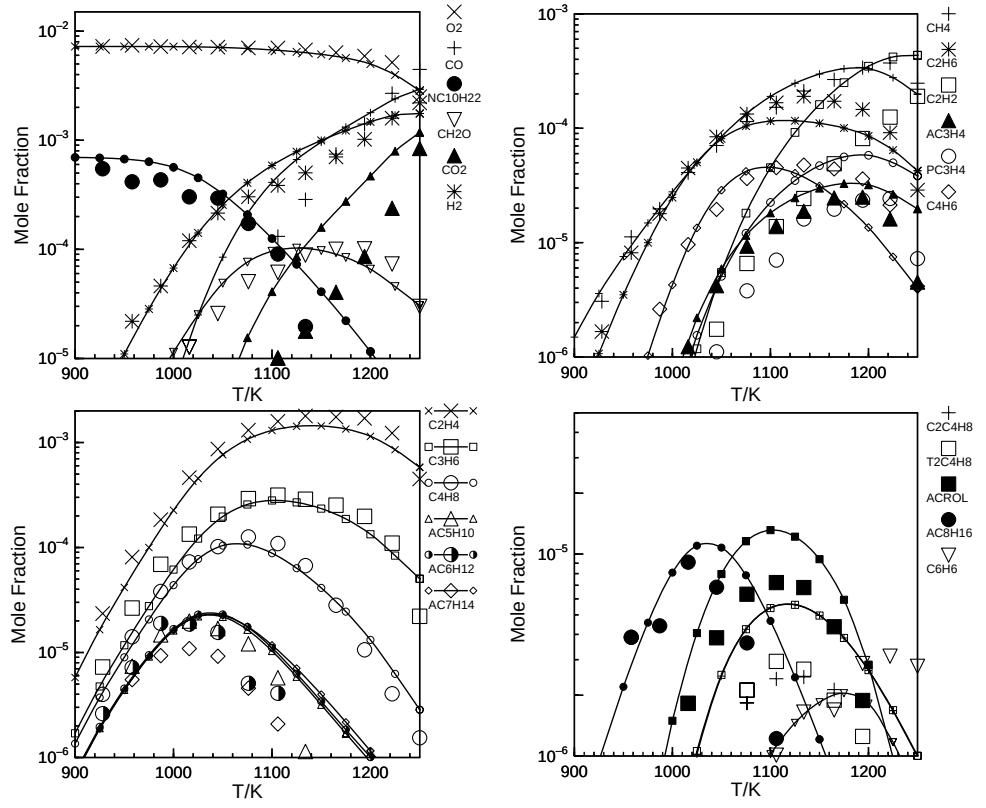

Fig. 3. The oxidation of *n*-decane in a JSR (700 ppmv of *n*-decane, 7230 ppmv of oxygen, nitrogen diluent; 0.07 s, 1 atm). The data (large symbols) are compared to the modeling (lines and small symbols).

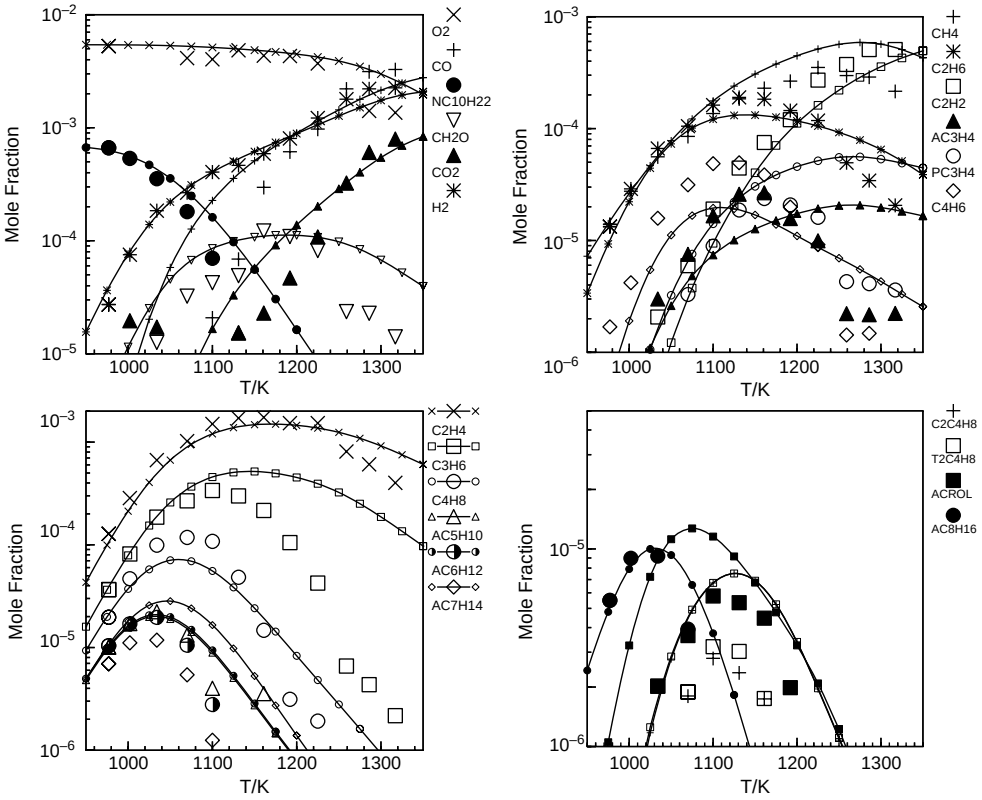

Fig. 4. The oxidation of *n*-decane in a JSR (700 ppmv of *n*-decane, 5425 ppmv of oxygen, nitrogen diluent; 0.07 s, 1 atm). The data (large symbols) are compared to the modeling (lines and small symbols).

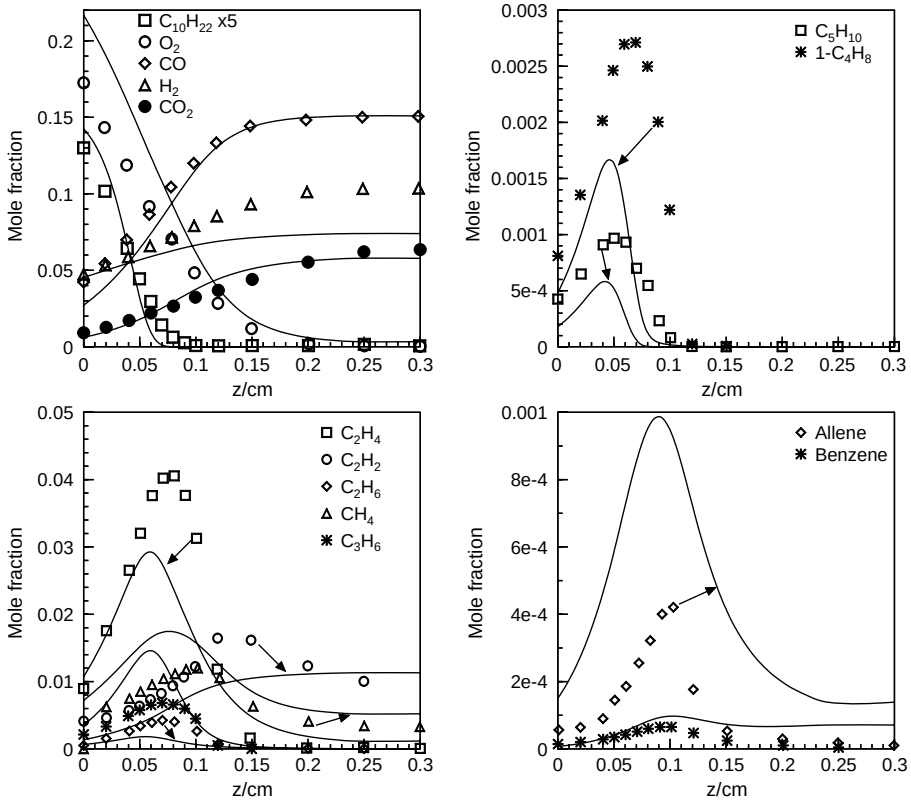

Fig. 5. The oxidation of *n*-decane under premixed flame conditions (1 atm, 0.01074033 g/cm^2/s, initial mole fractions: 0.0319 of *n*-decane, 0.2857143 of oxygen, 0.6823857 of nitrogen).The data of [4] (symbols) are compared to the modeling (lines).

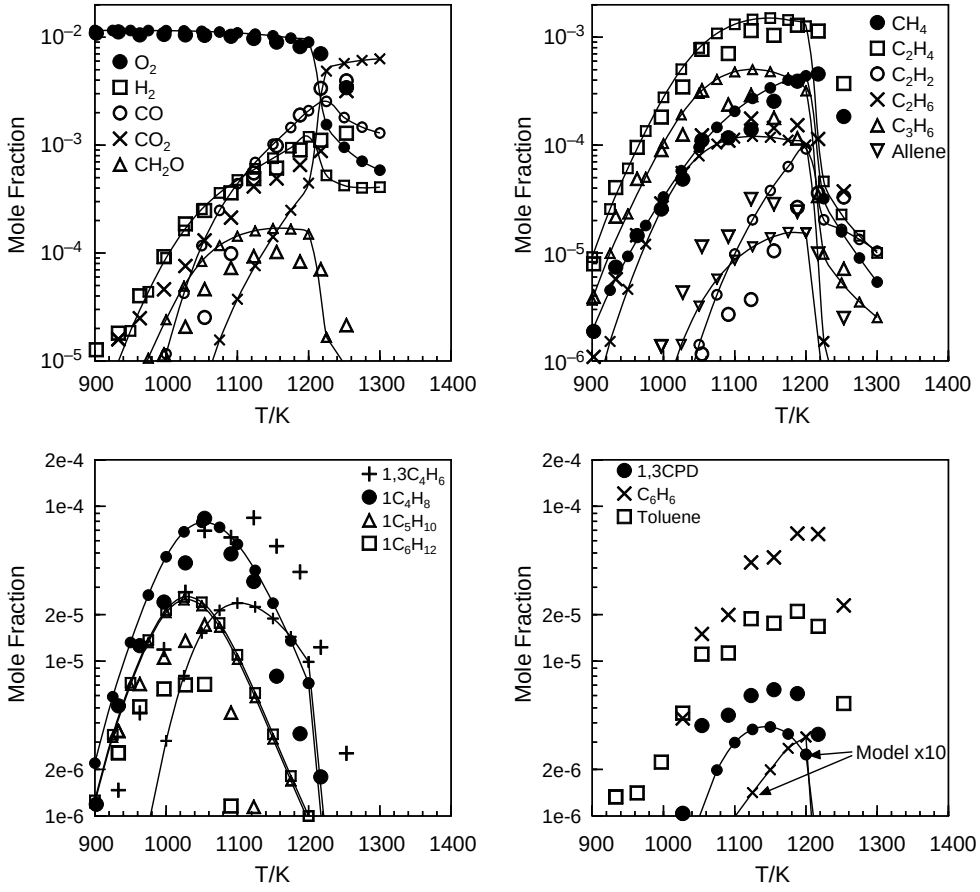

Fig. 6. The oxidation of kerosene in a JSR (700 ppmv of kerosene, 11,550 ppmv of oxygen, nitrogen diluent; 0.07 s, 1 atm). The data (large symbols) are compared to the modeling (lines and small symbols) using *n*-decane as a model fuel (770 ppmv of *n*-decane, 11,550 ppmv of oxygen).

4 cm diameter (30.5 cm^3) made of fused-silica (to minimize wall catalytic reactions), equipped with 4 nozzles of 1 mm ID for the admission of the gases which are achieving the stirring. A nitrogen flow of 100 L/h was used to dilute the fuel. As in our previous JSR studies [1–3,5,6], all the gases were preheated before injection in order to minimize temperature gradients inside the JSR. A regulated heating wire of $\sim$1.5 kW maintained the temperature of the reactor at the desired working temperature. The reactants were diluted by nitrogen ($<$50 ppm of O_2; $<$1000 ppm of Ar; $<$ 5 ppm of H_2), and mixed at the entrance of the injectors. High purity oxygen (99.995% pure) was used in these experiments. Kerosene Jet-A1 was sonically degassed before use. A piston pump (Isco 100DM) was used to deliver the fuel to an atomizer–vaporizer assembly maintained at 200 °C. Good thermal homogeneity along the whole vertical axis of the reactor was observed for each experiment by thermocouple (0.1 mm Pt–Pt/Rh 10% located inside a thin-wall silica tube) measurements (gradients $\geq$1 K/cm). The reacting mixtures were probe sampled by means of a fused-silica low pressure sonic probe. The samples (ca. 4–6 kPa) were taken at steady temperature and residence time. They were analyzed on-line by means of a GC–MS and off-line after collection and storage in 1 L Pyrex bulbs: Low vapor-pressure compounds were analyzed on-line whereas permanent gases and high vapor-pressure species were analyzed off-line. These experiments were performed at steady state, at a constant mean residence time, the reactants flowing continually in the reactor, varying stepwise the temperature of the gases inside the JSR. A high degree of dilution was used, reducing temperature gradients in the JSR and heat release (no flame occurred in the JSR).

Gas chromatographs (GC), equipped with capillary columns (Poraplot-U, Molecular Sieve-5A, DB-5 ms, DB-624, Plot Al_2O_3/KCl, Carboplot-P7), thermal conductivity detector (TCD) and flame ionization detector (FID), were used for stable species measurements. Compounds identifications were made through GC/MS analyses of the samples. An ion trap detector operating in electron impact ionization mode (GC/MS Varian Saturn) was used. As in our previous studies [5,6], CH_2O and CO_2 were measured by FID after hydrogenation on a Ni/H_2 catalyst connected to the exit of the GC column. A good repeatability of the measurements and a good carbon balance ($100 \pm 10\%$) were obtained in this series of experiments.

3. Modelling

For simulating the oxidation of *n*-decane and kerosene [4] in premixed flames, we used the Premix computer code [7]. For the JSR computations, we used the PSR computer code [8]. It computes species concentrations from the balance

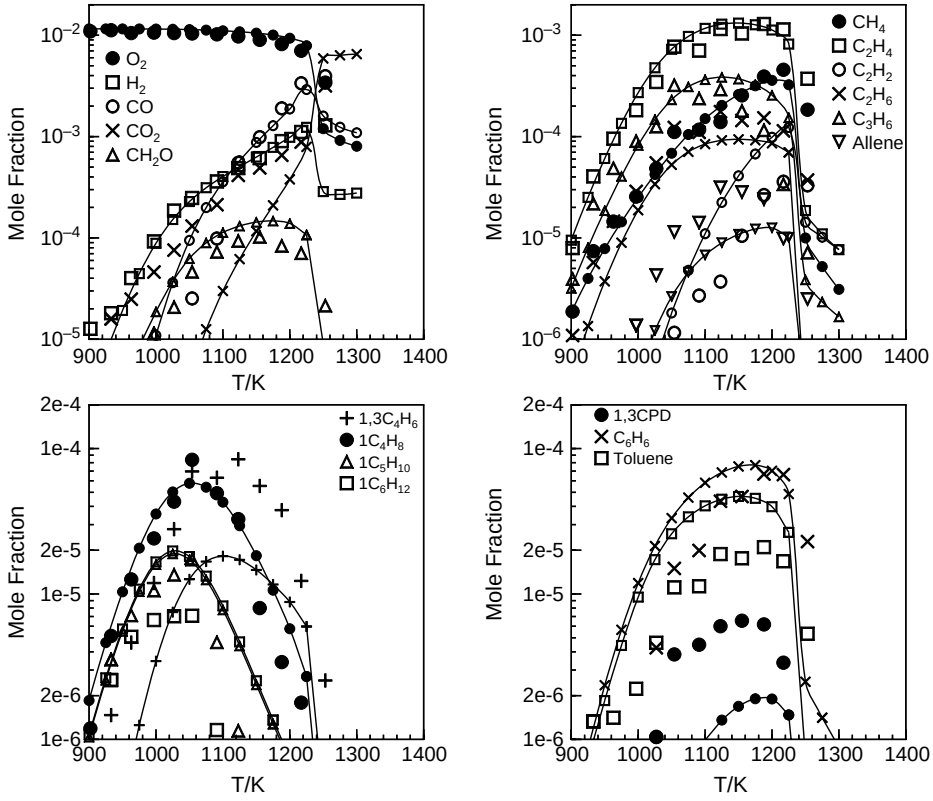

Fig. 7. The oxidation of kerosene in a JSR (700 ppmv of kerosene, 11,550 ppmv of oxygen, nitrogen diluent; 0.07 s, 1 atm). The data (large symbols) are compared to the modeling (lines and small symbols) using *n*-decane/*n*-propylbenzene as a model fuel (585 ppmv of *n*-decane, 206 ppmv of *n*-propylbenzene, 11,550 ppmv of oxygen).

between the net rate of production of each species by chemical reactions and the difference between the input and output flow rates of species. These rates are computed from the kinetic reaction mechanism and the rate constants of the elementary reactions calculated at the experimental temperature, using the modified Arrhenius equation: $k = AT^n \times \exp(-E/RT)$. The reaction mechanism used in this study has a strong hierarchical structure. It is based on the comprehensive commercial fuel oxidation mechanism developed earlier [9] where the rate expressions of pressure dependent reactions have been updated (Table 1). The reaction mechanism used here consisted of 209 species and 1673 reversible reactions. This mechanism, including references and thermochemical data, is available from the authors (dagaut@cnrs-orleans.fr). Since most of it has been presented in detail in previous papers [1,5,6], only the reaction of importance here will be described in the text. The rate constants for reverse reactions are computed from the corresponding forward rate constants and the appropriate equilibrium constants, $K_c = k_{forward}/k_{reverse}$, calculated using thermochemical data [10–12].

4. Results and discussion

4.1. The oxidation of n-decane in a JSR

Since *n*-decane is a key compound for the modelling of the oxidation of kerosene [1–3,13–15], new experiments were performed and modelled using a detailed kinetic reaction scheme. The experimental results consisted of the mole fractions of the reactants, stable intermediates and final products as a function of temperature. They are compared to PSR computational results in Figs. 1–4. These results confirm the already reported intermediate formation of simple olefins (mainly ethylene and propene), and methane representing the major intermediate hydrocarbons of *n*-decane oxidation [1,2,4,15–17]. As can be seen from Figs. 1–4, the kinetic model used here represents fairly well the experimental data.

4.2. The oxidation of n-decane in a premixed flame

The atmospheric pressure *n*-decane premixed flame of Douté et al. [4] was also simulated in the present study to further test the kinetic model. The experimental temperature profile reported by the authors was used in the computations. The results of the comparison between the experimental data and the modelling results are presented in Fig. 5. Again, a good agreement between data and the modelling was observed, further confirming the validity of our kinetic scheme. It is noticeable from Fig. 5 that the computed and experimental mole fraction profiles for *n*-decane, oxygen, CO, CO_2, and benzene are in very good agreement. However, the model tends to underestimate the maximum mole fractions of hydrogen, ethylene, acetylene, ethane, and to overestimate those of methane, propene, and allene. Since we were pretty confident

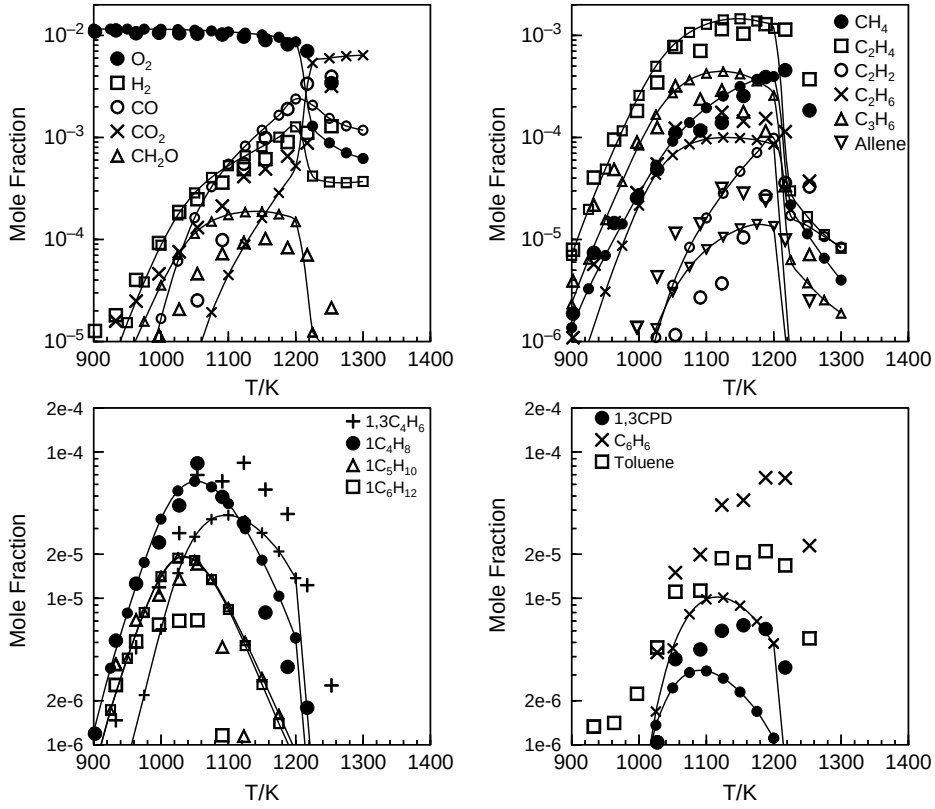

Fig. 8. The oxidation of kerosene in a JSR (700 ppmv of kerosene, 11,550 ppmv of oxygen, nitrogen diluent; 0.07 s, 1 atm). The data (large symbols) are compared to the modeling (lines and small symbols) using *n*-decane/*n*-propylcyclohexane as a model fuel (585 ppmv of *n*-decane, 206 ppmv of *n*-propylcyclohexane, 11, 550 ppmv of oxygen).

in this kinetic sub-scheme, it was included in the kerosene kinetic scheme used in the further computations.

4.3. The oxidation of kerosene in a JSR

As for *n*-decane, the experimental results consisted of the mole fractions of the reactants, stable intermediates and final products measured at fixed residence time, as a function of temperature. They are compared to PSR computational results in Figs. 6–12. These results confirm the already reported intermediate formation of simple olefins (mainly ethylene and propene) and methane representing the major intermediate hydrocarbons [1,2,4] formed from the oxidation of kerosene.

In order to test the effect of the composition of the model fuel on the modelling results, we simulated the oxidation of kerosene at stoichiometry using four different model fuels. The results of these tests are reported below.

4.3.1. n-Decane as a model fuel

As can be seen from Fig. 6, the modelling of kerosene oxidation in a JSR at stoichiometry using *n*-decane as a model fuel yields good agreement between the data and the modelling results for most of the species but 1,3-cyclopentadiene, benzene, and toluene, for which the model strongly under estimates the concentration. These results confirm the similitudes between *n*-decane and kerosene kinetics of oxidation already reported [1–4]. They also confirm the inclusion of non-paraffinic components in the model fuel is necessary to simulate the formation of aromatics [9].

4.3.2. n-Decane/n-propylbenzene as a model fuel

As can be seen from Fig. 7, the modelling of kerosene oxidation in a JSR in stoichiometric conditions using a *n*-decane/*n*-propylbenzene mixture (74%/26% mol) as a model fuel yields good agreement between the data and the modelling results for most of the species but 1,3-cyclopentadiene, benzene, and toluene. Actually, the mole fractions of benzene and toluene are overestimated whereas that of 1,3-cyclopentadiene are underestimated. These results confirm the inclusion of cycloalcanes in the model fuel is necessary [9].

4.3.3. n-Decane/n-propylcyclohexane as a model fuel

As can be seen from Fig. 8, the modelling of kerosene oxidation in a JSR in stoichiometric conditions using a *n*-decane/*n*-propylcyclohexane mixture (74%/26% mol) as a model fuel yields good agreement between the data and the modelling results for most of the species but benzene, and toluene. There, the mole fractions of benzene and toluene are strongly underestimated. This result was expected based on our previous results obtained from the oxidation of *n*-propylcyclohexane [5] showing little formation of benzene and toluene.

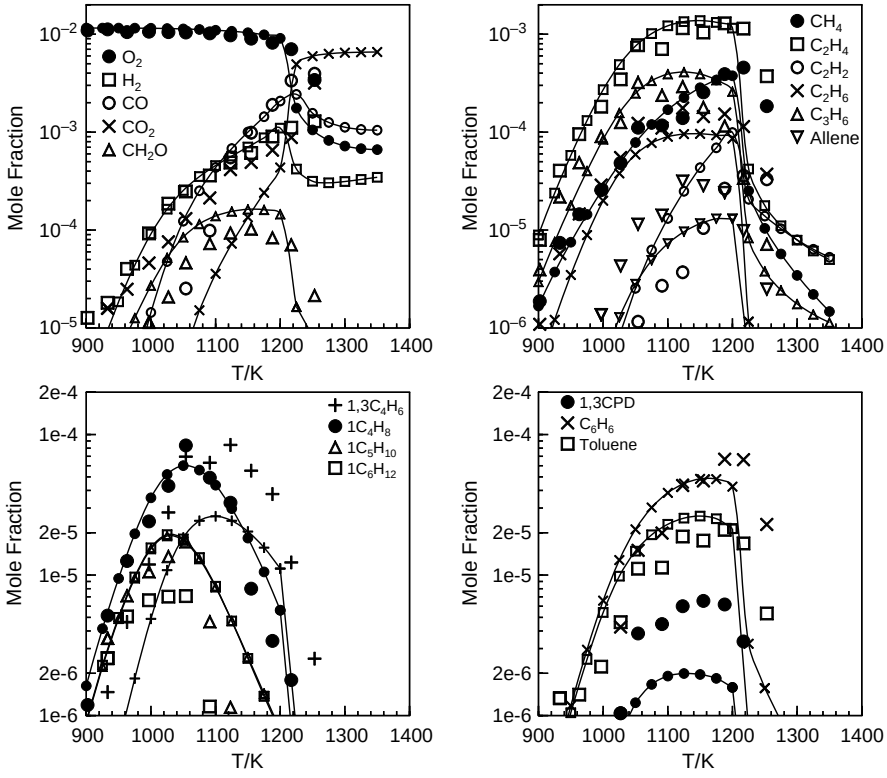

Fig. 9. The oxidation of kerosene in a JSR (700 ppmv of kerosene, 11,550 ppmv of oxygen, nitrogen diluent; 0.07 s, 1 atm). The data (large symbols) are compared to the modeling (lines and small symbols) using *n*-decane/*n*-propylbenzene/*n*-propylcyclohexane as a model fuel (585 ppmv of *n*-decane, 119 ppmv of *n*-propylbenzene, 87 ppmv of *n*-propylcyclohexane, 11,550 ppmv of oxygen).

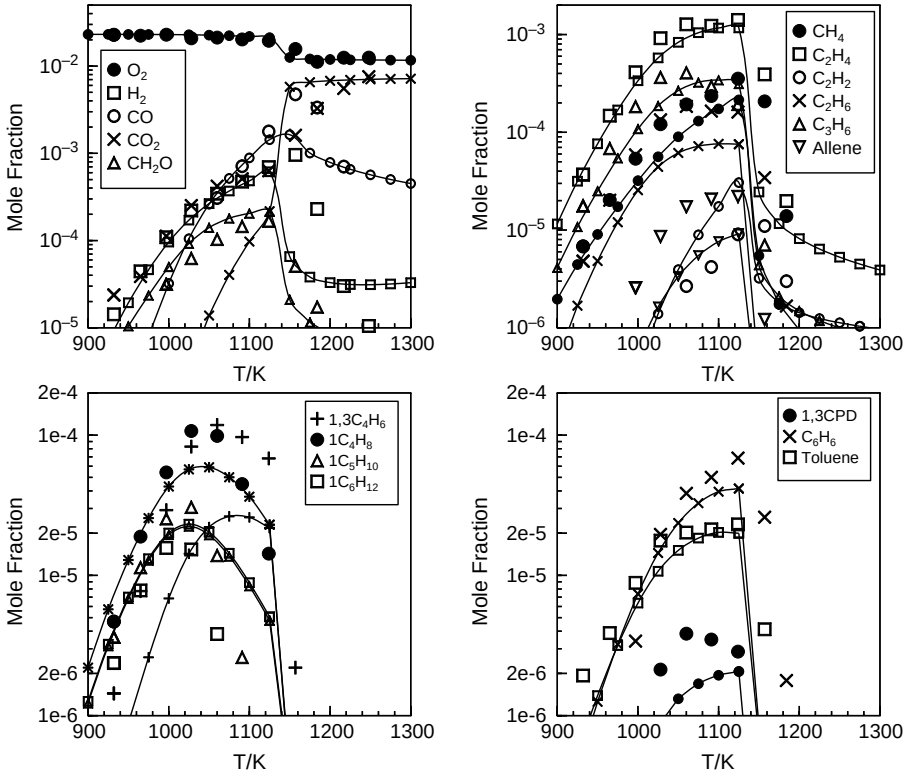

Fig. 10. The oxidation of kerosene in a JSR (700 ppmv of kerosene, 23,100 ppmv of oxygen, nitrogen diluent; 0.07 s, 1 atm). The data (large symbols) are compared to the modeling (lines and small symbols) using *n*-decane/*n*-propylbenzene/*n*-propylcyclohexane as a model fuel (585 ppmv of *n*-decane, 119 ppmv of *n*-propylbenzene, 87 ppmv of *n*-propylcyclohexane, 23,100 ppmv of oxygen).

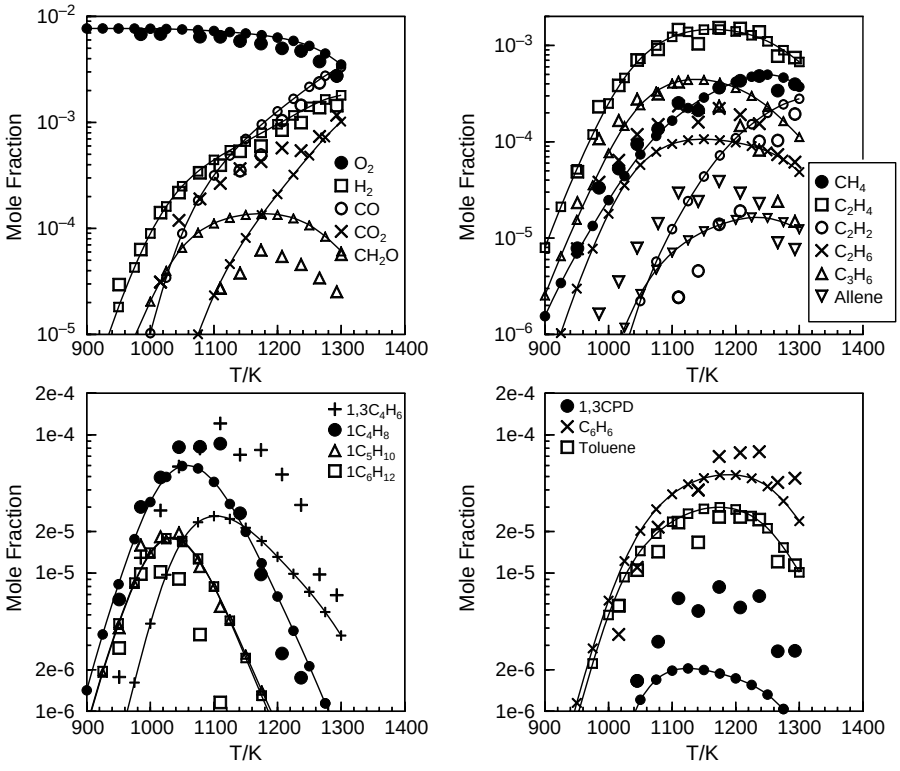

Fig. 11. The oxidation of kerosene in a JSR (700 ppmv of kerosene, 7700 ppmv of oxygen, nitrogen diluent; 0.07 s, 1 atm). The data (large symbols) are compared to the modeling (lines and small symbols) using *n*-decane/*n*-propylbenzene/*n*-propylcyclohexane as a model fuel (585 ppmv of *n*-decane, 119 ppmv of *n*-propylbenzene, 87 ppmv of *n*-propylcyclohexane, 7700 ppmv of oxygen).

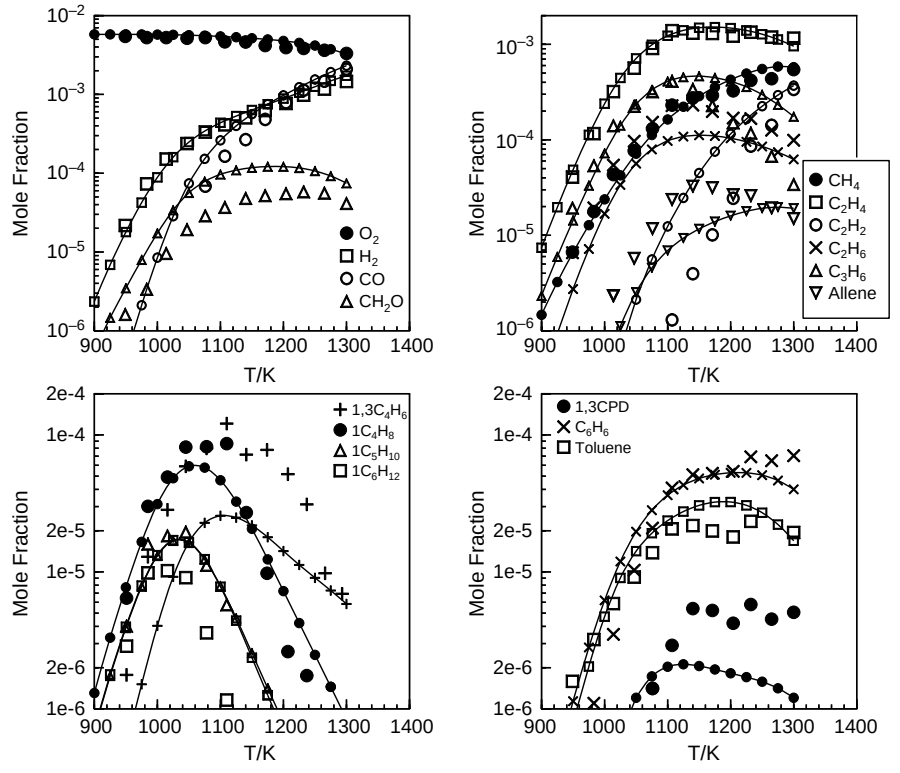

Fig. 12. The oxidation of kerosene in a JSR (700 ppmv of kerosene, 5775 ppmv of oxygen, nitrogen diluent; 0.07 s, 1 atm). The data (large symbols) are compared to the modeling (lines and small symbols) using *n*-decane/*n*-propylbenzene/*n*-propylcyclohexane as a model fuel (585 ppmv of *n*-decane, 119 ppmv of *n*-propylbenzene, 87 ppmv of *n*-propylcyclohexane, 5775 ppmv of oxygen).

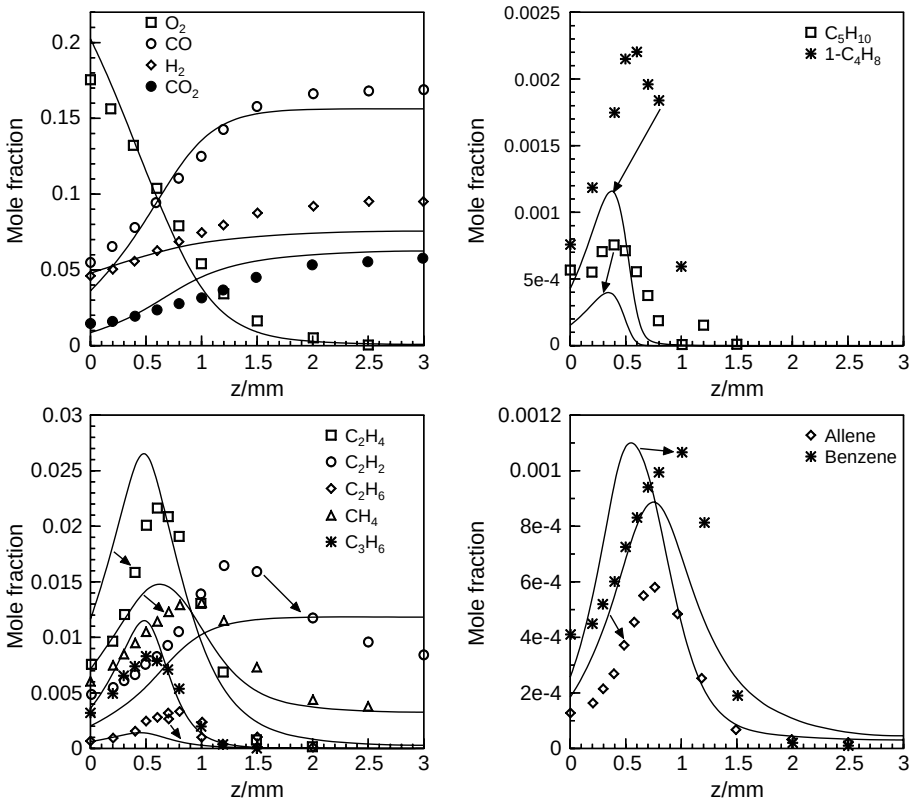

Fig. 13. The oxidation of kerosene under premixed flame conditions (1 atm, 0.010739794 g/cm^2/s, initial mole fractions: 0.0319 of kerosene, 0.28643 of oxygen).The data of [4] (symbols) are compared to the modeling (lines). Initial mole fractions in the modeling: *n*-decane, 0.02463685; *n*-propylbenzene, 0.004993912; *n*-propylcyclohexane, 0.003662271, oxygen, 0.28643; nitrogen, 0.680276967).

4.3.4. n-Decane/n-propylbenzene/ n-propylcyclohexane as a model fuel

A third model fuel composition was tested, more representative of the composition of kerosene. As can be seen from Fig. 9, the modelling of kerosene oxidation in a JSR in stoichiometric conditions using a *n*-decane/*n*-propylbenzene/*n*-propylcyclohexane (74%/14%/11% mol) mixture as a model fuel yields good agreement between the data and the modelling results for most of the species. This model is also able to satisfactorily predict the formation of simple aromatics. Therefore, this three-components model fuel was selected for modelling the other kerosene oxidation experiments performed using a JSR and a flat flame burner [4]. Figs. 10–12 further demonstrate that this three-component model fuel is satisfactory for modelling the oxidation of kerosene under JSR conditions.

A kinetic analysis of the reaction paths during the oxidation of the stoichiometric mixture indicates that the overall oxidation of the fuel is driven by *n*-decane. According to the model, at 900 K, where the oxidation of the fuel starts in the conditions of Fig. 9, OH radicals are the main species involved in the oxidation of the fuel mixture. The oxidation of *n*-decane is responsible for the production of these radicals via a complex reaction scheme that can be summarized as follows:

$$n-C_{10}H_{22} \Rightarrow 3-C_{10}H_{21},\ 3-C_{10}H_{21},\ 5-C_{10}H_{21}$$

$$n-C_{10}H_{22} \Rightarrow 1-C_8H_{17},\ 4-C_8H_{17},\ 2-C_8H_{17},\ 3-C_8H_{17}$$

The decyl and octyl radicals isomerize and decompose. Their decomposition yields 1-butyl radicals that in turn decompose. The further reactions in turn yield OH radicals.

$$1-C_4H_9 + M \Rightarrow C_2H_5 + C_2H_4 + M$$

$$C_2H_5 + O_2 \Rightarrow C_2H_4 + HO_2$$

$$2HO_2 \Rightarrow H_2O_2 + O_2$$

$$H_2O_2 + M \Rightarrow 2OH + M$$

$$CH_3 + HO_2 \Rightarrow OH + CH_3O$$

4.4. The oxidation of kerosene in a premixed flame

Douté et al.[4] measured the flame structure of an atmospheric pressure kerosene premixed flame using a flat flame burner, probe sampling and GC analyses. This flame was also simulated in this study to further check the validity of our kinetic model. In the computations we used the experimental temperature profile reported by the authors [4]. The three-component model fuel was used. The results of the comparison between the experimental data [4] and the modelling are presented in Fig. 13. A good agreement between data and the modelling was observed. This result further confirmed the

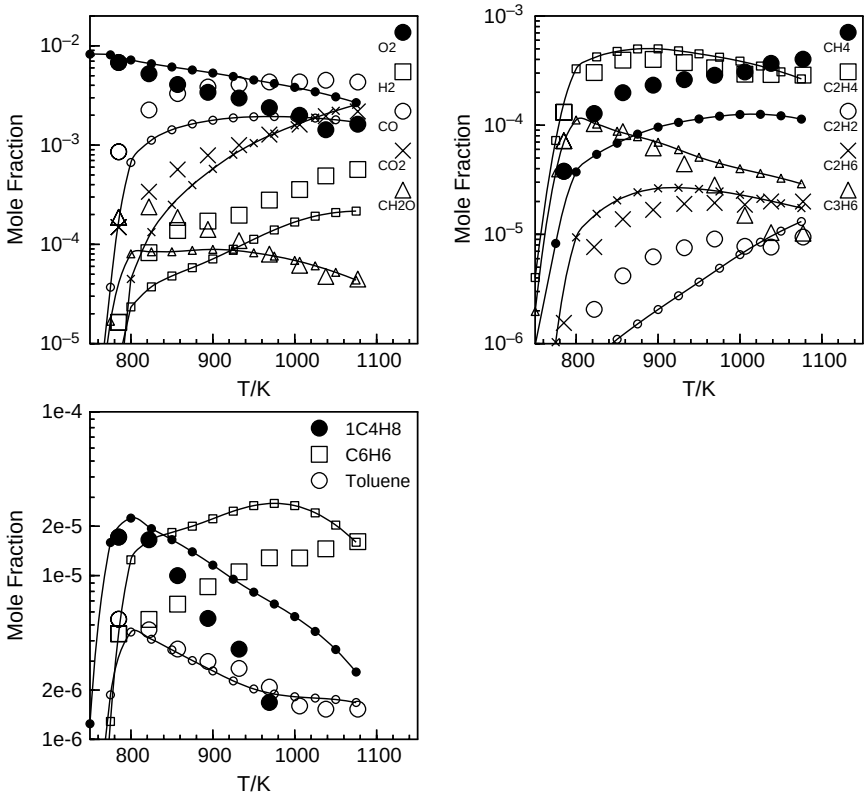

Fig. 14. The oxidation of kerosene in a JSR (500 ppmv of kerosene, 8250 ppmv of oxygen, nitrogen diluent; 1.0 s, 20 atm). The data (large symbols) are compared to the modeling (lines and small symbols) using *n*-decane/*n*-propylbenzene/*n*-propylcyclohexane as a model fuel (418 ppmv of *n*-decane, 85 ppmv of *n*-propylbenzene, 62 ppmv of *n*-propylcyclohexane, 8250 ppmv of oxygen).

validity of our kinetic scheme and the choice of the surrogate three-component model fuel. In this figure, it is noticeable that the computed and experimental mole fraction profiles for oxygen, hydrogen, CO, CO_2, allene, and benzene are in very good agreement. However, the model tends to underestimate the maximum mole fractions of acetylene and ethane, and to slightly overestimate those of methane, ethylene, and propene.

4.5. The oxidation of kerosene in a JSR under elevated pressure

The experimental results obtained earlier [1] for the oxidation of kerosene in diluted conditions and under elevated pressures in the range 10–40 atm were also modelled using this kinetic reaction mechanism. A reasonable agreement between the data obtained at 10, 20, and 40 atm, and the simulations was observed. An example of the comparison between the experimental results of [1] and the present modelling is given in Fig. 14, indicating the typical degree of agreement between data and simulation.

5. Conclusion

New experimental results were obtained for the oxidation of *n*-decane and kerosene in a JSR. These data were used in conjunction with *n*-decane and kerosene flame structures taken from the literature to validate a kinetic reaction scheme. Amongst the four surrogate kerosene model fuels used, the *n*-decane/*n*-propylbenzene/*n*-propylcyclohexane (74/14/11% in mol) mixture gave the best agreement with the JSR and flame data. The same scheme was used to successfully simulate the previously published results for the JSR oxidation of kerosene TR0 at 10, 20 and 40 atm [1].

Acknowledgements

Partial financial support from CEA is gratefully acknowledged. The authors are grateful to Dr M. Cathonnet for his interest in this work.

References

[1] Dagaut P, Reuillon M, Boettner J-C, Cathonnet M. Proc Combust Inst 1994;25:919.
[2] Dagaut P, Reuillon M, Cathonnet M, Voisin D. J Chim Phys Phys-Chim Biol 1995;92:47.
[3] Cathonnet M, Voisin D, Etsouli A, Sferdean C, Reuillon M, Boettner J-C. Symposium of the applied vehicle technology panel on gas turbine engine combustion, emissions and alternative fuels, Lisbon, Portugal, 12–16 October 1998, RTO Meeting Proceedings 1999;14:14.
[4] Douté C, Delfau J-L, Akrich R, Vovelle C. Combust Sci Technol 1995; 106:327.
[5] Ristori A, Dagaut P, El Bakali A, Cathonnet M. Combust Sci Technol 2001;165:197–228.
[6] Dagaut P, Ristori A, El Bakali A, Cathonnet M. Fuel 2002;81:173–84.
[7] Kee RJ, Grcar JF, Smooke MD, Miller JA. PREMIX: a Fortran program for modelling steady laminar one-dimensional premixed flame. Sandia

Report SAND85-8240. Livermore, CA: Sandia National Laboratories; 1985.
[8] Glarborg P, Kee RJ, Grcar JF, Miller JA. PSR: a Fortran program for modeling well-stirred reactors. Sandia Report No.SAND86-8209. Livermore, CA: Sandia National Laboratories; 1986.
[9] Dagaut P. Phys Chem Chem Phys 2002;4:2079–94.
[10] Tan Y, Dagaut P, Cathonnet M, Boettner J-C. Combust Sci Technol 1994; 102:21.
[11] Kee RJ, Rupley FM, Miller JA. Thermodynamic data base. Livermore, CA: Sandia National Laboratories; 1991.
[12] Muller C, Michel V, Scacchi G, Côme G-M. J. Chim Phys Phys-Chim Biol 1995;92:1154.
[13] Lindstedt, RP. Proc Combust Inst 1998;27:269–85.
[14] Mawid MA, Park TW, Sekar B, Arana C. AIAA 2004-4207. p. 1–25.
[15] Dagaut P, Cathonnet M. Prog Energy Combust Sci, in press.
[16] Delfau JL, Bouhria M, Reuillon M, Sanogo O, Akrich R, Vovelle C. Proc Combust Inst 1990;23:1567–72.
[17] Dagaut P, Reuillon M, Cathonnet M. Combust Sci Technol 1994;103: 349–59.